CHINESE OPTICS LETTERS

Vol. 19, No. 8 | August 2021

Fiber-based optical frequency comb at 3.3 μm for broadband spectroscopy of hydrocarbons [Invited]

Karol Krzempek[1*], Dorota Tomaszewska[1], Aleksandra Foltynowicz[2], and Grzegorz Sobon[1]

[1] Laser & Fiber Electronics Group, Faculty of Electronics, Wrocław University of Science and Technology, 50-370 Wroclaw, Poland

[2] Department of Physics, Umeå University, 901 87 Umeå, Sweden

*Corresponding author: karol.krzempek@pwr.edu.pl

Received April 22, 2021 | Accepted June 22, 2021 | Posted Online August 3, 2021

A 125 MHz fiber-based frequency comb source in the mid-infrared wavelength region is presented. The source is based on difference frequency generation from a polarization-maintaining Er-doped fiber pump laser and covers a spectrum between 2900 cm^{-1} and 3400 cm^{-1} with a simultaneous bandwidth of 170 cm^{-1} and an average output power up to 70 mW. The source is equipped with actuators and active feedback loops, ensuring long-term stability of the repetition rate, output power, and spectral envelope. An absorption spectrum of ethane and methane was measured using a Fourier transform spectrometer to verify the applicability of the mid-infrared comb to multispecies detection. The robustness and good long- and short-term stability of the source make it suitable for optical frequency comb spectroscopy of hydrocarbons.

Keywords: fiber laser; femtosecond laser; difference frequency generation; nonlinear frequency conversion.
DOI: 10.3788/COL202119.081406

1. Introduction

Laser absorption spectroscopy is a powerful tool for precise quantification of the composition of solids[1], liquids[2], and gases[3,4]. Proper sensor design allows for non-invasive measurements with high selectivity and sensitivity, which is required in numerous out-of-lab applications[5]. Mid-infrared (mid-IR) laser sources are commonly used in laser absorption spectroscopy to take advantage of high molecular absorption coefficients in this spectral region. Conventional gas detection techniques rely on using continuous wave (CW) mid-IR lasers targeting selected molecular transitions[6]. Due to the narrow tuning range of distributed feedback-type (DFB) semiconductor lasers, multi-gas analysis requires incorporating several individual sources in the sensor platform[7,8]. The other approach to simultaneous detection of several molecular species is based on broadband coherent sources. Optical frequency combs, which offer broad spectral coverage, high spectral coherence, and a direct link to RF standards[9], are particularly suited for multispecies trace gas detection.

The most common method of obtaining a mid-IR comb relies on frequency conversion of a near-IR mode-locked laser source by means of nonlinear techniques: optical parametric oscillator (OPO) and difference frequency generation (DFG). The OPOs can provide a multi-watt output combined with broad tunability[10], but, on the other hand, they require a phase lock of the cavity to the pumping laser. The DFGs are promising alternatives to OPOs due to their simplified design (a single-pass configuration instead of a cavity). Moreover, if both beams interacting in the DFG process originate from one pump laser, the generated mid-IR idler is free of the carrier-envelope offset frequency (f_{CEO}), which simplifies the absolute frequency stabilization of the comb. The 3 μm mid-IR spectral region, particularly interesting for spectroscopy due to the presence of strong absorption lines of numerous molecules, including hydrocarbons, can be accessed using DFG sources based on widely available periodically poled lithium niobate (PPLN) crystals. Mixing of 1.55 μm and 1.06 μm femtosecond pulses, generated from rare-earth-doped fiber lasers, enables us to obtain a broadband idler in the 3.3 μm region. For a fully passive cancellation of the f_{CEO}, a 3.3 μm DFG system must be seeded by a single near-IR frequency comb (either Yb- or Er-doped fiber-based). In the first case, an Yb-doped femtosecond laser is used to pump a highly nonlinear fiber (HNLF), which generates a signal red-shifted towards 1.5 μm via the Raman-induced soliton self-frequency shift (SSFS)[11–15]. This approach benefits from the broad tuning range of the solitons and, thus, a wide tunability of the idler. However, since mode-locked Yb-doped fiber lasers (YDFLs) require bulk grating compressors to deliver high-peak-power femtosecond pulses, the DFG setups presented so far required free-space coupling of the pump radiation to the nonlinear fiber. This necessitates the use of precise optomechanics, increases the overall complexity, and makes the system vulnerable to external disturbances. In order to avoid the free-space coupling of light to a very small core of the nonlinear fiber, one can use an Er-doped

fiber laser (EDFL) as seed for the DFG[16–19]. An EDFL can be designed as an entirely fiberized source of high-power femtosecond pulses at 1.56 μm without using bulk compressors. In this case, the HNLF is used for down-conversion of the 1.56 μm signal to the 1 μm band via dispersive wave (DW) generation[20]. Using this method, Zhu *et al.*[16] generated a frequency comb spanning from 2.9 to 3.6 μm with 120 mW of average power. Later, Meek *et al.*[17] presented a similar source generating 150 mW power centered at 3.1 μm. In Ref. [18], Cruz *et al.* presented an EDFL-based DFG covering the spectral range of 2.8–3.5 μm with 500 mW of average power. Very recently, an octave-spanning comb in the mid-IR with an average power of 29 mW was presented, with the use of an aperiodically poled Mg $LiNbO_3$ crystal[19]. However, none of these EDFL-based DFGs were fully stabilized in terms of output power and spectral envelope, by, e.g., using an active lock of the DFG pulse overlap. An alternative solution to avoid the active pulse overlap control in DFG is to use the intra-pulse DFG (IDFG) approach. In IDFG, a spectrally broad, few-cycle pulse is focused on a nonlinear crystal to form a broadband mid-IR idler[21–23]. Recently, a six-octave optical frequency comb was generated from an EDFL[24]. Nevertheless, IDFG sources suffer from relatively low output power (e.g., 3.5 mW in Ref. [24]).

Here, we present a robust, mid-IR comb source based on the DFG effect in a PPLN crystal, operating in the 3 μm range suitable for spectroscopy of hydrocarbons. The simple configuration requires a single EDFL as a seed source for both pump and signal generation. The seed laser and amplifiers are built all-in-fiber, so the setup is practically alignment-free. Moreover, active stabilization of crucial emission parameters [repetition frequency (f_{ref}) and average output power] is implemented to ensure the long-term stability of the emitted radiation. An absorption measurement of methane (CH_4) and ethane (C_2H_6) is presented to confirm the applicability of the mid-IR comb to multispecies detection.

2. Experimental Results

The experimental setup is depicted in Fig. 1. The heart of the source is a graphene mode-locked EDFL operating at a center wavelength of 1565 nm, generating 320 fs pulses at a repetition rate of ~125 MHz. To ensure stable operation of the EDFL, the laser cavity is temperature stabilized at 35°C, and a fiber piezoceramic stretcher (PZT) is used to control the f_{rep}. The f_{rep} is stabilized to an external RF reference. In Ref. [25], we showed that in a closed loop, the standard deviation (SD) of f_{rep} was less than 3 Hz for a 5 h measurement period and was limited by the stability of the RF source used as a reference. More details on the seed source and the f_{rep} stabilization method can be found in Ref. [25]. The EDFL seed pulses are divided in a fiber coupler and delivered to two separate branches. In the first branch (lower part of Fig. 1), the pulses are temporally stretched in a dispersion-compensating fiber, amplified to 77 mW in a custom-built Er-doped fiber amplifier (EDFA) and subsequently recompressed to 99 fs in a piece of polarization-maintaining single-mode fiber (PMF). In this part, a motorized fiber optical delay line and a PZT are added to allow precise adjustment of the optical length of this section. The spectrum of the compressed pulses along with the autocorrelation measurement is depicted in Fig. 2.

In the second branch of the source (upper part of Fig. 1), the 1565 nm pulses are boosted to 280 mW of average power and a 55 fs duration before reaching an HNLF, in which a DW generation process occurs. Note that the HNLF is spliced to the amplifier output and therefore does not require any alignment.

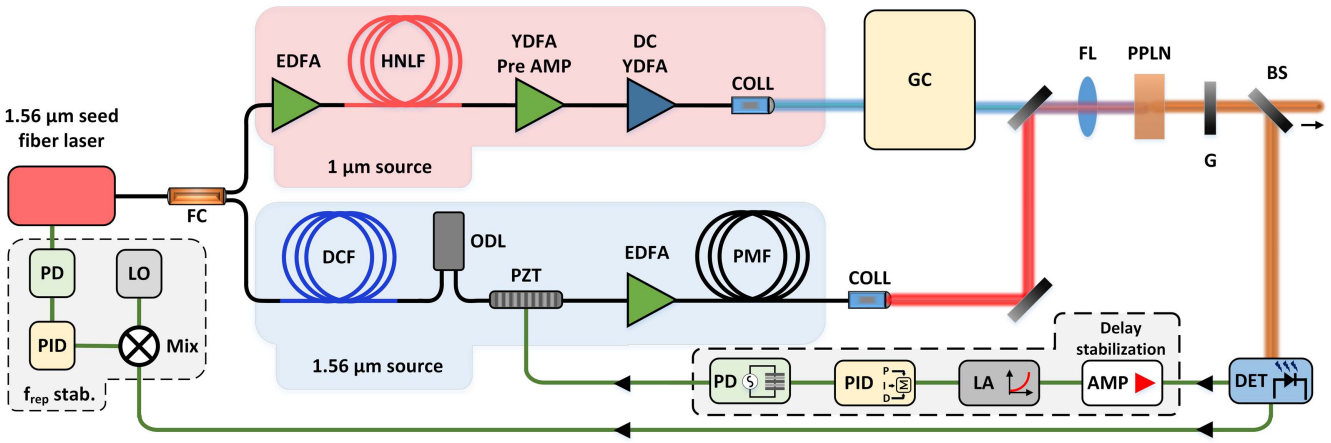

Fig. 1. Schematic of the fiber-based mid-IR comb source. PD, piezo driver; PID, proportional integral derivative controller; LO, local oscillator; Mix, RF mixer; FC, fiber coupler; EDFA/YDFA, Er- or Yb-doped fiber amplifier; HNLF, highly nonlinear fiber; DCF, dispersion compensating fiber; ODL, fiberized optical delay line; PZT, piezoceramic fiber stretcher; PMF, polarization-maintaining single-mode fiber; COLL, collimator; GC, grating compressor; FL, focusing lens; PPLN, 3-mm-long periodically poled lithium niobite crystal; G, germanium filter; BS, beam splitter; DET, MCT detector; AMP, RF amplifier; LA, logarithmic amplifier. Fibers are indicated in black, and electrical connections are in green.

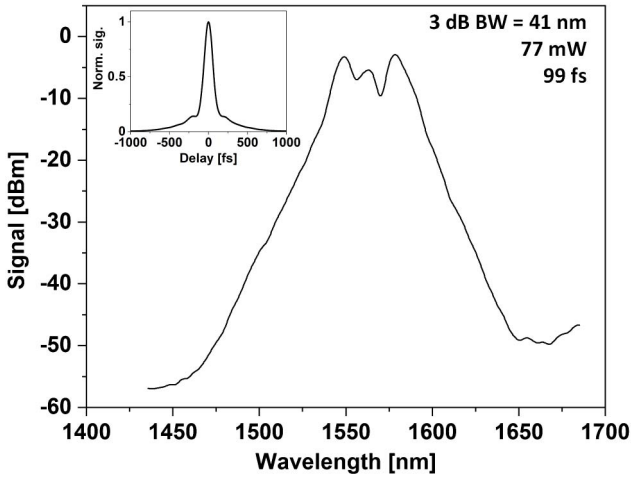

Fig. 2. Optical spectrum of the compressed 1565 nm pulses. The inset shows the measured autocorrelation trace.

As a result, broadband radiation centered at 1060 nm is achieved. Next, the DW is boosted in a custom-built Yb-doped pre-amplifier and subsequently in a double-clad Yb-doped amplifier. The 1060 nm pulses are then directed to a transmissive grating-based compressor (GC). At the output, the pulses have a 195 fs duration and reach 1.9 W of average power. The optical spectrum of the compressed 1 μm pulses along with the autocorrelation measurement is depicted in Fig. 3.

The pulses from the 1.56 μm branch and the 1 μm branch of the source are co-aligned on a dichroic mirror and directed through a 75 mm lens into a 3-mm-long PPLN crystal with five quasi-phase matching (QPM) periods (29.52–31.59 μm). Both branches of the source are designed and built so that their optical path lengths are equal. As a result of the nonlinear DFG process in the crystal, broadband radiation in the vicinity of 3.2 μm is generated. The emitted central wavelength can be tuned between 2900 cm^{-1} (3450 nm) and 3400 cm^{-1} (2940 nm) by switching

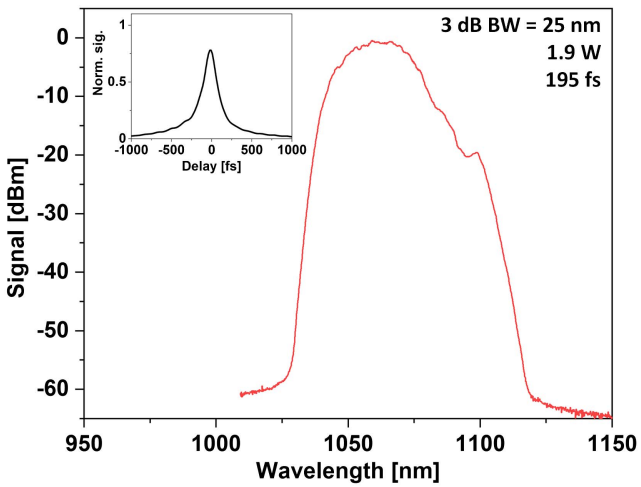

Fig. 3. Optical spectrum of the compressed 1 μm pulses. The inset shows the measured autocorrelation trace.

the PPLN crystal period, tuning its temperature, and adjusting the peak power of the pulses coupled into the HNLF, thus influencing the shape of the 1 μm DW spectrum. The tuning characteristics of the spectrum registered using a Fourier-transform spectrometer (FTS) are depicted in Fig. 4 (lower panel). The maximum 3 dB bandwidth (BW) of the generated radiation is 177 nm. The highest average output power equal to 70 mW was registered at a center wavelength of emission of 3200 cm^{-1}. The spectral coverage of the DFG source allows accessing strong transitions of numerous molecules, e.g., hydrocarbons CH_4, acetylene (C_2H_2), ethylene (C_2H_4), ethane (C_2H_6), and hydrogen chloride (HCl). The absorption spectra of those species are plotted in the upper panel of Fig. 4.

In femtosecond DFG sources, crucial parameters of the emitted radiation, e.g., the average output power and the shape of the spectral envelope, strongly depend on the temporal overlap between the pulses interacting in the nonlinear medium. Therefore, active stabilization of the 1 μm and 1.56 μm pulse overlap is obligatory for long-term repeatability, required, e.g., in broadband gas absorption spectroscopy applications. To stabilize the temporal overlap, we use the method demonstrated in Refs. [25,26], in which an error signal is obtained from the measurement of the relative intensity noise (RIN) in the idler. As shown in the lower part of Fig. 1, a part of the generated mid-IR beam is directed to a mercury cadmium telluride (MCT) detector, whose output voltage signal is low-pass filtered (f_{cut} = 20 MHz), amplified, and fed to a logarithmic amplifier (LA), which in turn converts the noise density in the registered signal to a DC voltage that acts as an error signal for a proportional integral derivative (PID) controller. The PID controller generates a correction signal for a PZT driver controlling the elongation of a stretch of the PMF, thus varying the optical path

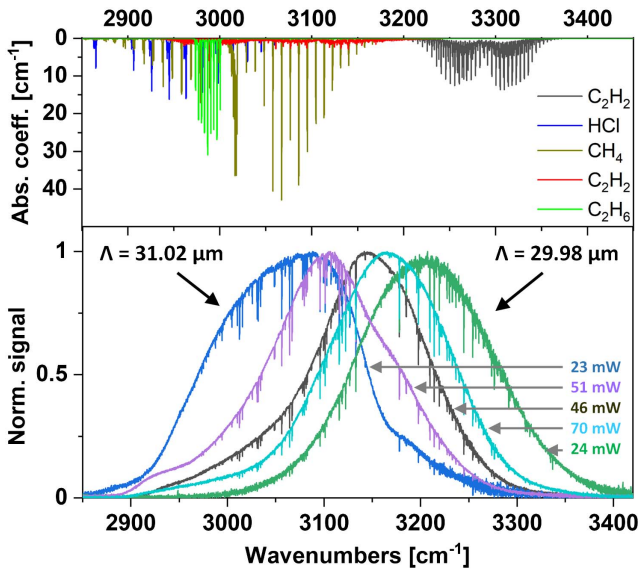

Fig. 4. Generated optical spectra for different PPLN crystal periods, with average output power indicated in each measurement. Absorption lines of several molecules within the spectral coverage of the source are depicted in the upper panel.

length of the 1565 nm pulses. A local minimum of the DC voltage signal delivered by the LA corresponds to a perfect overlap between the pulses taking part in the DFG process and simultaneously the maximum average output power.

The performance of the stabilization loop is depicted in Fig. 5. If no stabilization of the pulse overlap is employed, the spectral envelopes [Fig. 5(a)] and the average output power [Fig. 5(b)] fluctuate significantly during a 120 min period due to external perturbations (mostly temperature drift of the fibers). The active feedback loop used in our source compensates the thermal drift and ensures tight overlap of the pulses during long-term operation. After stabilizing the pulse overlap, the average output power fluctuation did not exceed a 1σ SD of 0.2 mW in 4.5 h, which is four times better compared to the non-stabilized case. The impact of the active feedback loop can also be seen in the stability of the generated spectrum, which did not vary significantly during the 4.5 h measurement period.

To verify the usability of the mid-IR comb source in gas spectroscopy applications, a proof-of-concept experiment was conducted, in which the broadband laser was used to detect absorption lines of CH_4 and C_2H_6 located near 3250 nm. The DFG source was tuned to this wavelength, and the beam was sent through two 10-cm-long cells filled with 615 ppm (parts per million) C_2H_6 in N_2 at 200 Torr (1 Torr = 133.322 Pa) and 0.245% CH_4 at 760 Torr, respectively. The transmitted light was sent into a home-built FTS with a balanced detector based on MCT photodiodes. The design of the FTS is similar to the

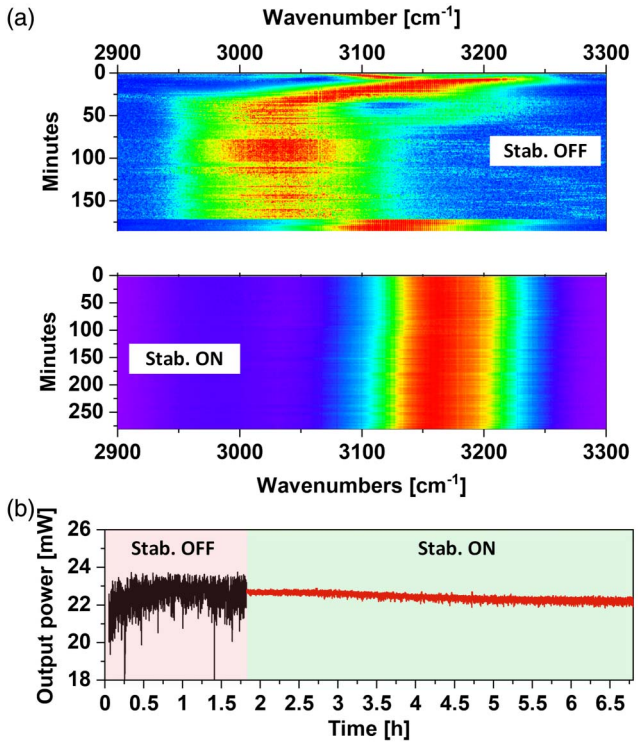

Fig. 5. (a) Heatmaps showing the time evolution of the spectrum for non-stabilized and stabilized cases. (b) Average output power stability as a function of time.

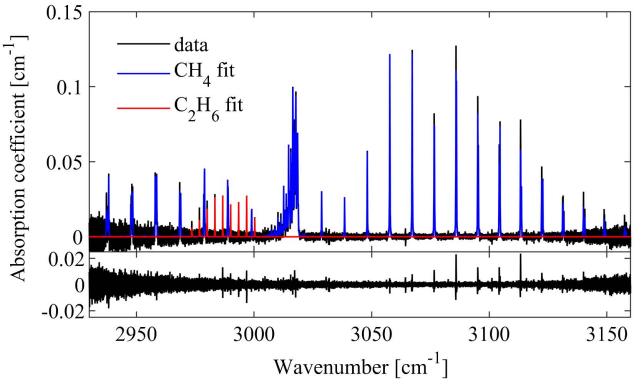

Fig. 6. Absorption spectrum of CH_4 and C_2H_6 measured using the DFG comb and a Fourier transform spectrometer (black) compared to the spectra of the two molecules (blue and red). The residuum of the fit is shown in the lower panel.

one in Ref. [27]. The optical path difference was calibrated using a 1.55 μm laser diode, whose beam was co-propagating with the comb beam in the FTS. The spectral resolution of the FTS was set to 125 MHz. A set of 100 interferograms was acquired with and without the absorption cells in the beam path. The fast Fourier transforms (FFTs) of the interferograms were averaged, and the absorption spectrum was normalized to the background spectrum in order to produce the transmission spectrum. Figure 6 shows in black the absorption coefficient calculated from the transmission spectrum using the Lambert–Beer law. The blue and red curves show the fitted models of the absorption coefficients of CH_4 and C_2H_6 calculated under the pertinent experimental conditions using the Voigt profile and the line parameters from the HITRAN 2016 database[28]. The gas concentrations were the only fitting parameters, and the baseline remaining after the normalization process was removed using the cepstral method[29]. The residuum of the fit is shown in the lower panel of Fig. 6, demonstrating excellent agreement between the experimental data and the model.

3. Conclusions

In this paper, a fully stabilized, tunable mid-IR DFG comb source is presented. The source is built using commercially available components in an all-PMF configuration and uses a single mode-locked EDFL as a seed. Tuning of the source parameters (temperature and QPM period of the crystal and the spectral position of the DW) enables covering the spectrum between 2900 cm^{-1} and 3400 cm^{-1} with a 3 dB BW up to 177 nm and average output power of 70 mW. The f_{rep}, average output power, and the spectral envelope were actively stabilized. The output power instability did not exceed 1σ SD of 0.2 mW during a 4.5-h-long measurement period. A proof-of-concept experiment confirmed that the constructed PMF-based mid-IR source can be used in broadband gas absorption spectroscopy applications.

Acknowledgement

This work was supported by the Foundation for Polish Science within the First TEAM program co-financed by the European Union under the European Regional Development Fund (No. First TEAM/2017-4/39). AF acknowledges the Knut and Alice Wallenberg Foundation (No. KAW 2015.0159).

References

1. W. M. Yen and P. M. Selzer, *Laser Spectroscopy of Solids* (Springer Science & Business Media, 2013).
2. V. Lazic and S. Jovićević, "Laser induced breakdown spectroscopy inside liquids: processes and analytical aspects," Spectrochim. Acta B At. Spectrosc. **101**, 288 (2014).
3. Y. Ma, A. Vicet, and K. Krzempek, "State-of-the-art laser gas sensing technologies," Appl. Sci. **10**, 433 (2020).
4. B. Fu, C. Zhang, W. Lyu, J. Sun, C. Shang, Y. Cheng, and L. Xu, "Recent progress on laser absorption spectroscopy for determination of gaseous chemical species," Appl. Spectrosc. Rev. (2020).
5. R. W. Solarz and J. A. Paisner, *Laser Spectroscopy and Its Applications* (Routledge, 2017).
6. Z. Du, S. Zhang, J. Li, N. Gao, and K. Tong, "Mid-infrared tunable laser-based broadband fingerprint absorption spectroscopy for trace gas sensing: a review," Appl. Sci. **9**, 338 (2019).
7. A. Genner, P. Martín-Mateos, H. Moser, and B. Lendl, "A quantum cascade laser-based multi-gas sensor for ambient air monitoring," Sensors **20**, 1850 (2020).
8. K. Krzempek, G. Dudzik, A. Hudzikowski, A. Gluszek, and K. Abramski, "Highly-efficient fully-fiberized mid-infrared differential frequency generation source and its application to laser spectroscopy," Opto-Electron. Rev. **25**, 269 (2017).
9. N. Picqué and T. W. Hänsch, "Frequency comb spectroscopy," Nat. Photon. **13**, 146 (2019).
10. F. Adler, K. C. Cossel, M. J. Thorpe, I. Hartl, M. E. Fermann, and J. Ye, "Phase-stabilized, 1.5 W frequency comb at 2.8–4.8 μm," Opt. Lett. **34**, 1330 (2009).
11. T. W. Neely, T. A. Johnson, and S. A. Diddams, "High-power broadband laser source tunable from 3.0 μm to 4.4 μm based on a femtosecond Yb:fiber oscillator," Opt. Lett. **36**, 4020 (2011).
12. T. A. Johnson and S. A. Diddams, "Mid-infrared upconversion spectroscopy based on a Yb:fiber femtosecond laser," Appl. Phys. B **107**, 31 (2012).
13. A. Ruehl, A. Gambetta, I. Hartl, M. E. Fermann, K. S. E. Eikema, and M. Marangoni, "Widely-tunable mid-infrared frequency comb source based on difference frequency generation," Opt. Lett. **37**, 2232 (2012).
14. G. Soboń, T. Martynkien, P. Mergo, L. Rutkowski, and A. Foltynowicz, "High-power frequency comb source tunable from 2.7 to 4.2 μm based on difference frequency generation pumped by an Yb-doped fiber laser," Opt. Lett. **42**, 1748 (2017).
15. L. Jin, V. Sonnenschein, M. Yamanaka, H. Tomita, T. Iguchi, A. Sato, K. Nozawa, K. Yoshida, S.-I. Ninomiya, and N. Nishizawa, "3.1–5.2 μm coherent MIR frequency comb based on Yb-doped fiber laser," IEEE J. Sel. Top. Quantum Electron. **24**, 0900907 (2018).
16. F. Zhu, H. Hundertmark, A. A. Kolomenskii, J. Strohaber, R. Holzwarth, and H. A. Schuessler, "High-power mid-infrared frequency comb source based on a femtosecond Er:fiber oscillator," Opt. Lett. **38**, 2360 (2013).
17. S. A. Meek, A. Poisson, G. Guelachvili, T. W. Hänsch, and N. Picqué, "Fourier transform spectroscopy around 3 μm with a broad difference frequency comb," Appl. Phys. B **114**, 573 (2014).
18. F. C. Cruz, D. L. Maser, T. Johnson, G. Ycas, A. Klose, F. R. Giorgetta, I. Coddington, and S. A. Diddams, "Mid-infrared optical frequency combs based on difference frequency generation for molecular spectroscopy," Opt. Express **23**, 26814 (2015).
19. L. Zhou, Y. Liu, H. Lou, Y. Di, G. Xie, Z. Zhu, Z. Deng, D. Luo, C. Gu, H. Chen, W. Li, and W. Li, "Octave mid-infrared optical frequency comb from Er:fiber-laser-pumped aperiodically poled Mg: $LiNbO_3$," Opt. Lett. **45**, 6458 (2020).
20. X. Liu, A. S. Svane, J. Lægsgaard, H. Tu, S. A. Boppart, and D. Turchinovich, "Progress in Cherenkov femtosecond fiber lasers," J. Phys. D Appl. Phys. **49**, 023001 (2016).
21. C. Gaida, M. Gebhardt, T. Heuermann, F. Stutzki, C. Jauregui, J. Antonio-Lopez, A. Schülzgen, R. Amezcua-Correa, A. Tünnermann, I. Pupeza, and J. Limpert, "Watt-scale super-octave mid-infrared intrapulse difference frequency generation," Light Sci. Appl. **7**, 94 (2018).
22. K. Liu, K. Liu, H. Liang, H. Liang, S. Qu, S. Qu, W. Li, W. Li, X. Zou, X. Zou, Y. Zhang, and Q. J. Wang, "High-energy mid-infrared intrapulse difference-frequency generation with 5.3% conversion efficiency driven at 3 μm," Opt. Express **27**, 37706 (2019).
23. J. Zhang, K. Fritsch, Q. Wang, F. Krausz, K. F. Mak, and O. Pronin, "Intrapulse difference-frequency generation of mid-infrared (2.7–20 μm) by random quasi-phase-matching," Opt. Lett. **44**, 2986 (2019).
24. D. M. B. Lesko, H. Timmers, S. Xing, A. Kowligy, A. J. Lind, and S. A. Diddams, "A six-octave optical frequency comb from a scalable few-cycle erbium fibre laser," Nat. Photon. **15**, 281 (2021).
25. K. Krzempek, D. Tomaszewska, A. Głuszek, T. Martynkien, P. Mergo, J. Sotor, A. Foltynowicz, and G. Soboń, "Stabilized all-fiber source for generation of tunable broadband f_{CEO}-free mid-IR frequency comb in the 7–9 μm range," Opt. Express **27**, 37435 (2019).
26. V. S. de Oliveira, A. Ruehl, P. Masłowski, and I. Hartl, "Intensity noise optimization of a mid-infrared frequency comb difference-frequency generation source," Opt. Lett. **45**, 1914 (2020).
27. A. Foltynowicz, T. Ban, P. Masłowski, F. Adler, and J. Ye, "Quantum-noise-limited optical frequency comb spectroscopy," Phys. Rev. Lett. **107**, 233002 (2011).
28. I. E. Gordon, L. S. Rothman, C. Hill, R. V. Kochanov, Y. Tan, P. F. Bernath, M. Birk, V. Boudon, A. Campargue, K. V. Chance, B. J. Drouin, J.-M. Flaud, R. R. Gamache, J. T. Hodges, D. Jacquemart, V. I. Perevalov, A. Perrin, K. P. Shine, M.-A. H. Smith, J. Tennyson, G. C. Toon, H. Tran, V. G. Tyuterev, A. Barbe, A. G. Császár, V. M. Devi, T. Furtenbacher, J. J. Harrison, J.-M. Hartmann, A. Jolly, T. J. Johnson, T. Karman, I. Kleiner, A. A. Kyuberis, J. Loos, O. M. Lyulin, S. T. Massie, S. N. Mikhailenko, N. Moazzen-Ahmadi, H. S. P. Müller, O. V. Naumenko, A. V. Nikitin, O. L. Polyansky, M. Rey, M. Rotger, S. W. Sharpe, K. Sung, E. Starikova, S. A. Tashkun, J. V. Auwera, G. Wagner, J. Wilzewski, P. Wcisło, S. Yu, and E. J. Zak, "The HITRAN2016 molecular spectroscopic database," J. Quantum Spectrosc. Radiat. Transf. **203**, 3 (2017).
29. R. K. Cole, A. S. Makowiecki, N. Hoghooghi, and G. B. Rieker, "Baseline-free quantitative absorption spectroscopy based on cepstral analysis," Opt. Express **27**, 37920 (2019).